Qatar Univ. Sci. J. (1995), 15 (1): 205 - 214

MINERALOGICAL AND GEOCHEMICAL EVALUATION OF UPPER CRETACEOUS BLACK SHALES, SAFAGA DISTRICT, EGYPT

By

H. HOLAIL*, M. ABD ALLA** AND M. EL DAHHAR**

* Department of Geology, Faculty of Science, University of Qatar, Doha, Qatar

** Department of Geology, Faculty of Science, Mansoura University, Mansoura, Egypt

التقييم المعدني والجيوكيميائي لصخور الطفلة السوداء بعصر الطباشيري العلوي في سفاجا بمصر

حنفي هليل و ممدوح عبد الله و محمد الدحار

بدراسة الخصائص الصخرية والتركيبية لصخور الطفله السوداء واالبريت (متكون حنوى) بالصحراء الشرقية - مصر وجد أن تركيبها المعدني والجيوكيميائي وكذلك نسبة نظائر الكربون المستقرة بهذه الصخور مشابه لمثيلتها من الرواسب الحديثة الغنية بالمواد العضوية . حيث أن الطفله السوداء تحتوي علي المكونات التالية : معادن طينية ، كوارتز ، مواد عضوية ، بيريت ، أصداف الفورامينفرا الجيرية وكذلك عقد فوسفاتية .

واتضح من الدراسة أن معادن الطين المكونة لطفله متكون حنوى لاتختلف عن مثيلتها من صخور الطفله السوداء المنتمية للعصر الطباشيري العلوي حيث أن معدني السمكثيت والاليت . كذلك توجد تركيزات عاليه من العناصر الشحيحة التي ترتبط بالتركيزات العالية للمواد العضوية .

ومن دراسة نسب نظائر الكربون المستقر اتضح أن هذه المواد العضوية ذات أصل قاري وبحري .

وتوضح العلاقة ما بين الكربون العضوي الكلي وتحتوي الكبريت تشابه بين صخور الطفله السوداء والرواسب البحرية حيث أن عنصر الحديد يعتبر أحد العوامل المتحكمة في تكوين معدني البيريت المصاحب للطفله السوداء .

Key Words : Upper Cretaceous, Safaga District, Lithofacies, Organic matter

ABSTRACT

Lithologic and compositional properties of black shale and pyrite from the Upper Cretaceous phosphorite/black shale deposits (Duwi Formation) of Eastern Desert of Egypt indicate similarity in mineralogy, geochemical characters and carbon isotopic ratios with those inferred for modern organic-carbon-rich sediments. Components of the black shale include various clay minerals, silt(grade quartz, organic matter, pyrite, calcareous foraminifera shells and phosphatic nodules.

The clay mineralogy of the black shale does not differ significantly from typical Cretaceous black shale (dominance of smectite and illite with minor amounts of kaolinite and chlorite).

The trace-element concentrations (Zn, Cu, Ni, Co, U and Pb) show a general enrichment pattern and seem to correlate with enrichment of organic matter. The stable carbon-isotope cratios (from- 22% to - 28.7 %) suggest that the organic matter is of continental and marine origin.

The relationship between the total organic carbon and sulfur contents of black shale samples is similar to that of marine sediments, but the pyrite content is probably controlled by the Fe^{2+} contents.

INTRODUCTION

Sediments rich in organic carbon are likely to be deposited in the modern oceans only where biological production in the waters is high, sediment accumulation rates and the burial rates are high, where organic matter is preserved in anoxic bottom waters. In general, black shales acquire their trace element contents from a variety of sources, including seawater, continental clastics and submarine vents. Scavenging by organic particles, complexation by organic matter, dissolution of oxide coatings and reprecipitation in reducing environments are important mech-

anisms [1-3]. Reliable data for many trace elements have been generated only within the last decade [4-7].

The occurrence of pyrite in black shales has been used to study the diagenetic history of black shale-pyrite associations [8-11]. It has become clear that the availability of reactive Fe^{2+}, metabolizable organic matter, and dissolved pore water sulfate play variable roles in controlling the distribution and diagenetic formation of pyrite [8, 12, 13, 14]. In anoxic marine sediments, sulfate-reducing bacteria convert sulfate to hydrogen sulfide, which reacts with reduced iron to form an initial iron monosulfide phase (Fe S).Pyrite precipitation appears to take place in anoxic marine sediments via reaction of the iron monosulfide with partially oxidized sulfur species and often results in a framboidal texture [15]. The reactivity of the organic matter in the marine sediments is particularly important because it limits the activity of sulfate-reducing bacteria [16]. As a consequence, the concentration of pyrite in marine sediments appears to be related in a simple way to the organic-carbon content.

Herein we focus on the mineralogy, geochemistry and the formation of iron sulfide minerals in Upper Cretaceous black shales of the Eastern Desert, Egypt. Geochemical characteristics of the black shale and the enclosed pyrite were used in order to evaluate the role of the various factors that controlled deposition and diagenesis of the Upper Cretaceous black shale and the timing of diagenetic sulfide formation.

TRATIGRAPHIC SETTING AND SEDIMENTOLOGICAL CHARACTERISTICS

Phosphorite/black shale deposits (Duwi Formation) of Late Cretaceous age are found in the Safaga-Quseir region along the Red Sea coast, Egypt (Fig. 1). The sedimentary sequence of the Duwi Formation has received considerable attention from sedimentologists [17-22]. The Duwi Formation is considered by Youssef [23] to be of Campanian age in the basal part and of Maastrichtian age in its upper part. This formation conformably overlies the Quseir variegated shale and conformably lies below the Dakhla shale [24].

The Upper Cretaceous black shale is a thin terrigenous bed within the phosphorite. This bed averages 1.2 m in thickness and ranges from fossiliferous, calcareous silty shale to mudstone. Shales are often found to contain small phosphatic grains which, in hand specimen, appear white to brown in color. The occurrence of silty layers and, occasionally, phosphorites indicate that sedimentation was variable. Although steady-state diagenetic conditions may have prevailed on the time scales represented by individual samples, the whole sequence is characterized by non-steady state conditions.

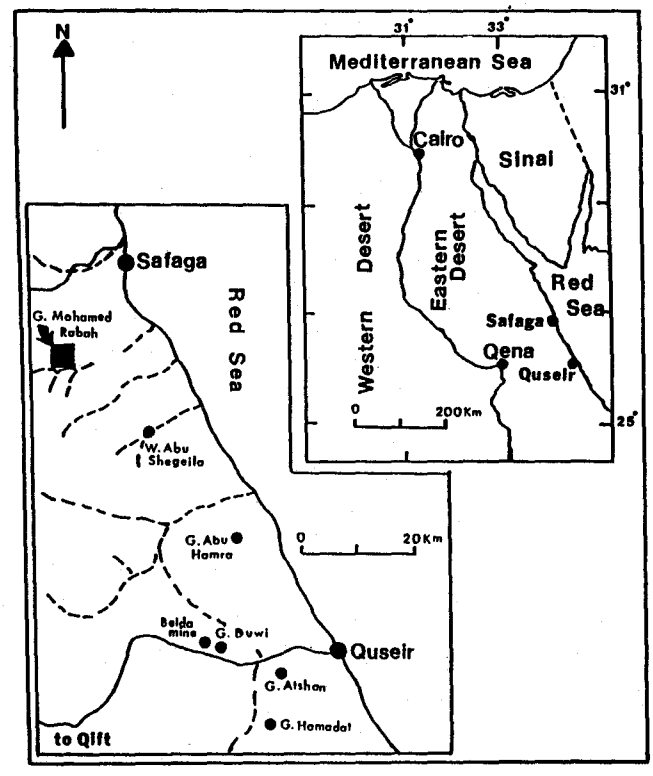

Figure 1. Location map with the position of the study area.

The fossiliferous shale contains a diverse, normal marine shelly fauna. The shale was deposited in a variety of facies, all below normal wave base, but well within the photic zone and mostly within well-oxygenated bottom waters. The presence of a diverse and locally abundant shelly fauna indicates that redox conditions were initially aerobic and initial sulfate reduction occurred only in reducing microenvironments. The pyrite occurs as small to medium crystals. Several varieties are present, including cubes, octahedra and pyritohedra, of which cubes by far are the most abundant. Isolated large pyrite cubes (1.0 cm in size) are abundant in some samples. Clusters of small pyrite spheroids displaying "framboidal texture" are occasionally seen. Framboidal texture is characteristic of pyrite which formed early in the depositional history and has been detected in numerous modern marine environments [8, 25]. There is no field evidence of epigenetic sulfide mineralization in the studied black shale

ANALYTICAL TECHNIQUES

The study samples were collected from the unweathered part of Upper Cretaceous Phosporite sequence at the Eastern Desert of Egypt (Fig. 1). Overall 60 samples were examined to represent all variations in color difference, carbonaceous material abundance, pyrite frequency and mineralogic composition. Some samples were disaggregated and wet sieved to concentrate sulfide minerals.

The isolated pyrite as well as the shale samples were analyzed by three principal techniques: 1) petrographic micro-

scope to document the texture of these samples, 2) scanning electron microscope (SEM) equipped with a link back-scattered electron (BSE) detector, and 3) X-ray diffraction to determine the mineralogical composition of shale samples.

Shale, as well as, pyrite samples were crushed and further ground by hand inan agate mortar. Major elements were determined by X-ray fluorescence (XRF) spectrometry using the fusion methods of Norrish and Hutton [26]. The trace elements were also determined by XRF using pressed powder samples. The sulfur content was determined gravimetrically. The sulfur assumed to be totally pyritic, as the organic sulfur content of the studied sediments would be insignificantly small, and evaporites are absent. Total organic carbon (TOC) was determined, in the insoluble residue form (1:1) HCI after filtering, drying and weighing the residue, by combustion in an electric furnace.

Determination of the stable carbon isotope ratios of the organic carbon of the studied black shale samples was under taken using a VG Micromass 602 mass (University of Michigan) calibrated with NBS-20 (carbonate) and NBS-21 (graphite) standards. Data are corrected for ^{17}O and are presented relative to the PPB standard.

RESULTS AND DISCUSSION

Lithofacies description

Three lithofacies were recognized in the studied Upper Cretaceous black- shale sequence: silt-rich mudstones, foraminifera-rich shales, and clay- and organic matter-rich black shales. These facies consist of components derived, in varying proportions, from different sources. The allochthonous components were derived from the surrounding landmass and consist of silt-grade quartz, detrital clays, and continental organic matter. The autochthonous components consist of biogenic carbonate, phosphate, and marine organic matter. The diagenetic components consist of pyrite, siderite, authigenic clay minerals, and organic matter.

a- Silt-rich mudstones. Hand specimens of this facies are typically of pale gray color and sometimes contain abundant bivalve shells. In thin section (Fig. 2A), this facies contains abundant silt-grade quartz (average 18%, range 3 - 27%) preserved in a matrix composed of clay and organic matter. The silt-rich mudstones are less organic-rich than the black shales (average 0.9%, range 0.2% 1.1%). Most of the silt-rich mudstones are nonlaminated. The presence of bivalve shells coupled with the absence of lamination and

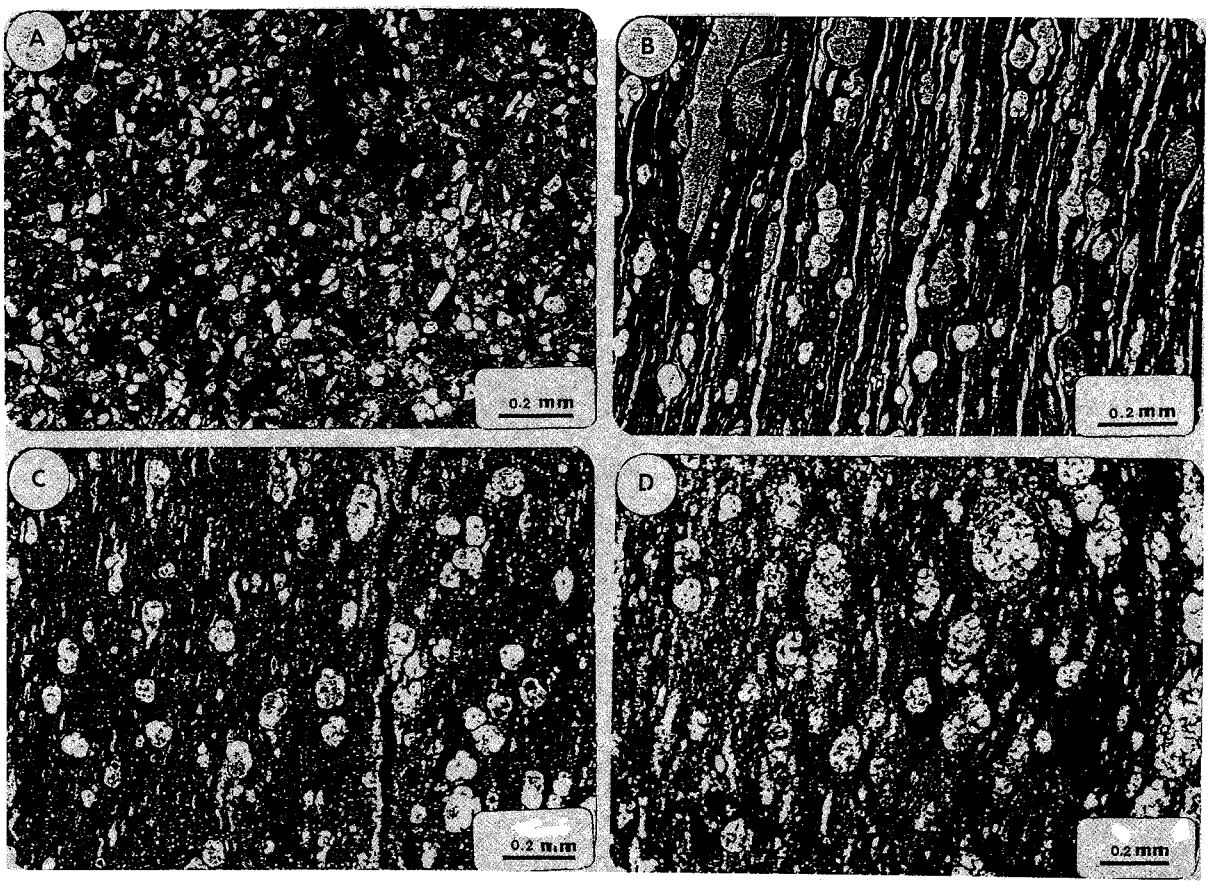

Figure 2. Photomicrographs of Upper Cretaceous black shales. A- Non-laminated, silt-rich mudstones. Dark material is amorphous organic matter. B- Laminated, foraminifera-rich shales. Calcareous foraminifera shells and phosphate nodules in a fine-grained clay matrix. C- Calcareous foraminifera shells. D- Quartz-replaced calcareous foraminifera shells.

pyrite in the silt-rich mudstone facies suggests that they were deposited in areas where the bottom water was suitable for colonization by organisms and was well-oxygenated [11].

b- Foraminifera-rich shales. -This facies has a range in composition, where it is dominated by calcareous foraminifera shells and phosphate nodules (Fig. 2B). This facies rarely shows any sedimentary structures other than bioturbation. In hand specimen, phosphate nodules appear white to brown in color. In thin section, this facies shows evidence of microlamination. Normally, the foraminifera - rich shale facies is carbonate rich. A significant proportion of the carbonate material in this facies is composed of calcareous foraminifera shells (Fig. 2C). The foraminifera shells and the phosphate nodules are scattered throughout the matrix. The matrix is composed of fine-grained clay (smectite, illite and kaolinite), organic matter and a small amount of pyrite. Detrital quartz is relatively uncommon. Diagenetic carbonate (siderite) may be present within the foraminifera tests (Fig. 2C) and as a pore-filling.

Based on estimates from thin sections, the foraminifera shells seldom exceed 12% of the rock volume. The skeletal microstructure is preserved, shells are composed of calcite and/or quartz-replaced calcite, with one composition usually dominating in a given thin bed (Figs. 2C & 2D). Quartz-replaced calcareous foraminifera shells typically consist of several quartz crystals in the size range of 12 - 30 μm. The chambers of these calcareous foraminifera are filled with micro-quartz crystals (Fig. 2D).

c- Clay and organic matter- rich black shales. In the field, this facies is dark gray to black and upon weathering tends to break up into small lath-shaped fragments. Petrographic analyses reveal that this facies is not laminated and is composed predominantly of clay which, as will be seen later, comprises smectite, illite, kaolinite, and chlorite. This facies is more rich in organic matter than the silt-rich mudstones (average 2.6%). The pyrite occurs both as framboids and as clusters of cubic forms.

Mineralogy

Smectite is the predominant clay species encountered in the studied black shales (Figs. 3 & 4). Smectite forms 50-80% of the clay assemblage. Other species, illite, kaolinite, and chlorite are generally scarce but locally present in considerable amounts (Fig. 3). The smectite displays anhedral

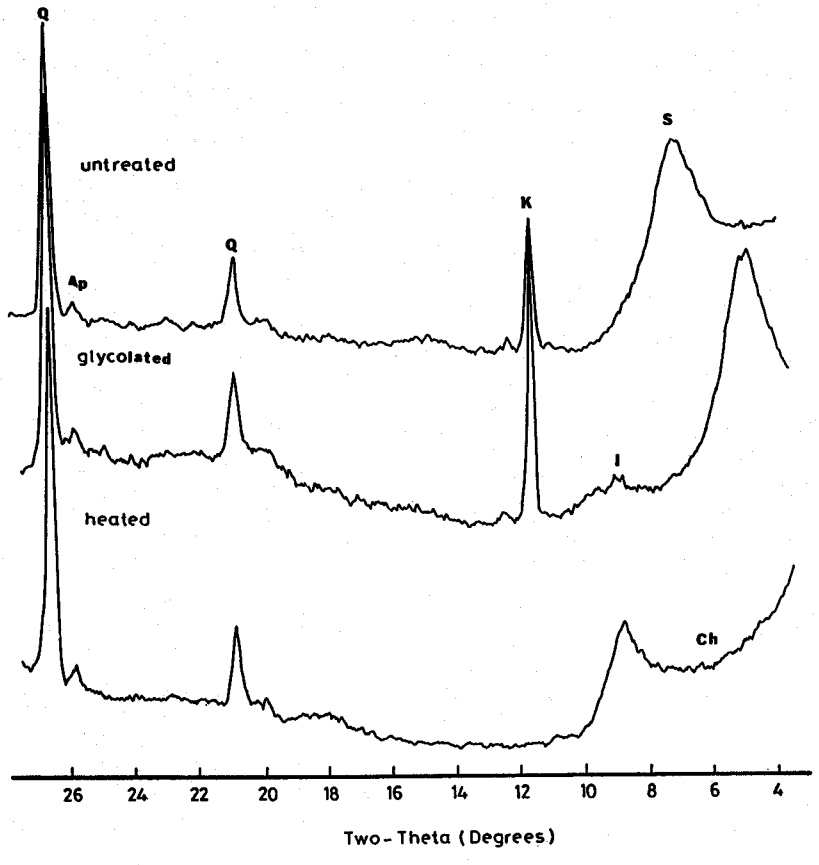

Figure 3. Representative X-ray diffractogram patterns of clay from Upper Cretaceous black shales.

flakes (Fig. 4A) and constitutes the bulk of the black-shale matrix. The illite shows two types of morphologies: anhedral flakes and euhedral filaments (Fig. 4B). The illite flakes are commonly associated with the smectite ones in the black shale matrix, while the filaments are observed in pores of all analyzed samples (Fig. 4B). The illite filaments are abundant in silt-rich mudstone facies but are rare in the black shale facies. In general, the black shale is overwhelmingly composed of smectite and illite with flaky morphology, and the silt-rich mudstone facies are rich in illite with both morphologies. Kaolinite occurs as booklets filling the pores of the analyzed samples (Fig. 4C). In some samples, the kaolinite cement comprises up to 6 percent of the total rock volume. Chlorite-illite cement showing a honeycomb type texture and fills the intergranular porosity.

Associated non-clay minerals include quartz, pyrite, phosphate, calcite, and siderite, diversely distributed in the black-shale bed (Figs 2, 4 & 5). There is no relationship between the variations in clay mineralogy and the lithology of the black-shale beds. In the same way, the clay assemblages do not depend on the abundance of organic matter, and do not differ systematically in black-shale facies.

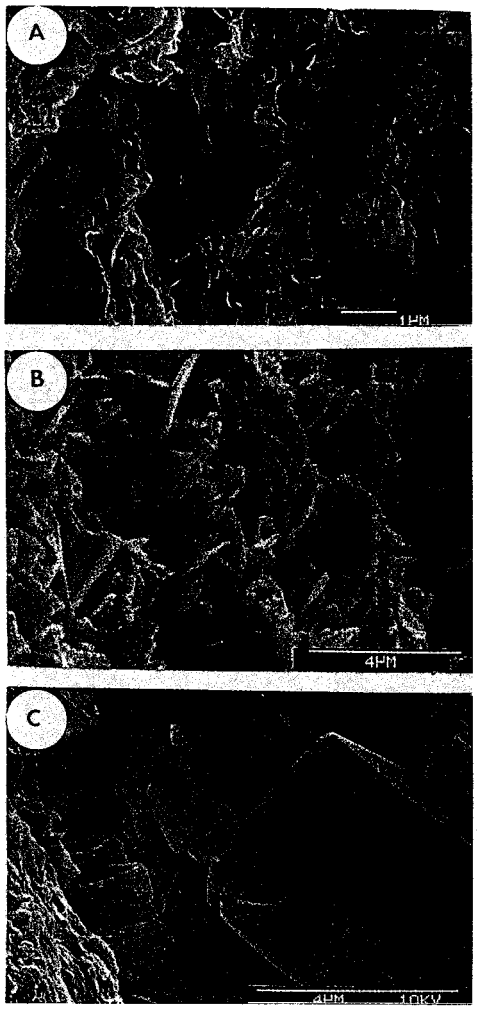

Figure 4. SEM photomicrographs of Upper Cretaceous black shales. A- Anhedral flakes of smectite. B- Illite showing two types: flakes and filaments. C- Booklets of kaolinite and large carbonate crystal filling the pores of the analyzed samples.

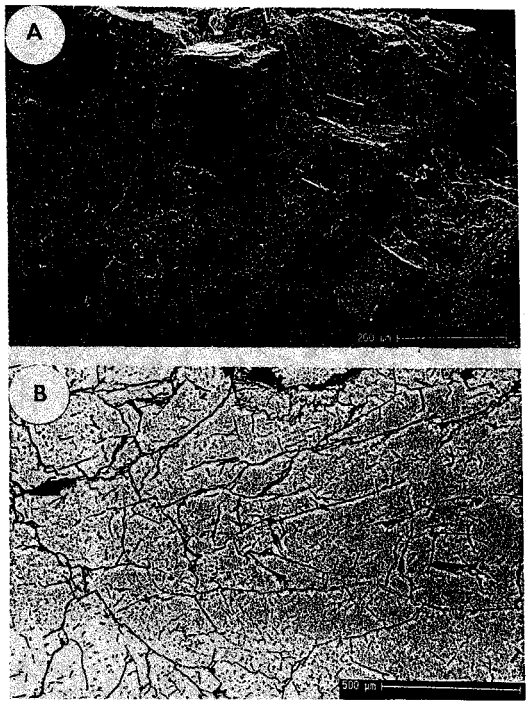

Figure 5. A- SEM photomicrograph of clustered pyrite crystals. B- Back-scattering photomicrograph of clustered pyrite crystals.

Geochemistry

The studied Upper Cretaceous black shales were originally argillaceous sediments containing organic matter. Their chemical composition has therefore been affected by numerous factors, including physicochemical conditions, prevailing organisms, the chemical composition of the water during deposition and the composition of detrital flux materials. The concentration ranges of the investigated major elements are tabulated in Table 1.

Table (1)

Range of major lment concentrations (wt%) in the black shales

Oxides	Range
Si_2O	51.1 - 68.2
Al_2O_3	9.1 - 16.4
TiO_2	0.6 - 0.8
Fe_2O_3	6.8 - 14.4
MnO	0.01 - 0.09
MgO	0.9 - 1.7
CaO	0.8 - 1.5
Na_2O	0.5 - 1.1
K_2O	0.9 - 1.2
P_2O_5	0.2 - 0.4

The SiO_2, Al_2O_3, MgO and Ti_2O are present in slightly low concentrations (mean 56.2%, 11.4%, 1.3% and 0.7%, respectively) because of dilution by organic matter. A few samples which are organic matter-poor show higher concentrations of SiO2, Al2O3, MgO and Ti_2O (mean 66%, 15.2%, 2.1% and 0.9%, respectively). These oxides are predominantly of terrigenous origin and therefore, reflect the abundant aluminosilicates. The K2O and Na2O contents are not unusually high. As expected, SiO_2, K_2O, Ba, Ni and Y are positively correlated, whereas SiO2, Co, Cu, Ga and Zn are negatively correlated. Al_2O_3 and TiO_2 concentrations show a good correlation (r = 0.9). The CaO and P_2O_5 contents are present in relatively high concentrations (mean 1.2% and 0.3%, respectively) due to the presence of the calcareous foraminifera shells and the phosphatic nodules. Total organic carbon and sulfur are considerably enriched in the studied Upper Cretaceous black shales, Fe is mostly present as pyrite. MnO (mean 0.07%) is depleted due to reductive mobilization.

The ranges of trace-element concentrations of the studied Upper Cretaceous black shales are given in Table 2. These element concentrations show a general enrichment relative to those given to shales by Ronov and Migdisov [27] and Cameron and Garrels [28]. Such enrichment can be related

Table (2)
Range of trace clcment conentrations in the black shalc and pyrite samples

	Ba	Ce	Co	Cr	Cu	Ni	Żn	Zr	Pb	Rb	Sr	G a	La	Y	Th	U
Black	199	54	12	131	22	72	62	234	12	21	198	11	26	28	7	2
shale	-	-	-	-	-	-	-	-	-	-	-	-	-	-	-	-
	344	94	30	238	45	92	134	431	21	37	253	21	45	44	12	5
Pyrite	29		13	13	77	29	11	14		5	10				2	4
	-	-	-	-	-	-	-	-	-	-	-	-	-	-	-	-
	142		30	30	114	52	41	27		13	25				10	7

to the paleoenvironmental conditions during black shale deposition or to diagenetic processes. It is generally recognized that organic matter is responsible for trace- element enrichment [29]. Calvert [30] thought that the cause of Pb, Cu, Mo, Zn, Ni and U enrichment in the south West Africa black muds was metal sorption on to degraded organic matter. In this study, the general enrichment pattern of Zn, Cu, Ni, Co, U and Pb seems to be associated with the presence of organic matter. Meanwhile, Cr and to a lesser extent Pb, Ni and Co may become enriched in the black shales as a result of remobilization.

In the studied black shales, Ba vs Zr, Rb vs Sr, Co vs Ga, Cr vs Zr, Ga vs La, Cu vs Ga, Y vs Ce, Co vs Zn, Cu vs La and Ga vs. Zn are positively correlated at high significant levels, whereas Cr vs Zn, Ba vs Ca, Ba vs Zn, Ga vs Ni, Ga vs Y, Th vs U, Ca vs Co and Ni vs Zn are negatively correlated; some of these relations are shown in Figure 6. Sr is clearly calcite- and phosphate-associated because of the highly significant correlation with CaO (r = 0.89). Both Pb and Cu correlate with Fe_2O_3 (pyrite) at highly significant levels (r = 0.81 and r = 0.78, respectively). The elements Rb, Y, Ba, Ga and Ce do not change significantly and for them a detrital, mainly clay-mineral origin may be confidently suggested.

Carbon isotopes

Sources of organic matter found in the studied black shale samples can be indicated by stable carbon isotope ratios. In modern sediments, land-derived organic matter is generally more depleted in ^{13}C than is marine organic matter. In general, continental C-3 plants synthesize organic matter having $\delta\ ^{13}C$ values ranging between -23.0 % and -33.0 %, whereas marine organic matter has values between -17.0 % and -23.0 % [31-32].

Carbon-isotope ratios of the organic carbon of the studied shale samples range between -22.0 % and -28.7 %, which is not a broad variation considering the considerable contrasts in organic-matter contents and lithologic types. A weak trend toward heavier carbon isotope with more marine isotopic compositions exists in some samples. Little difference in carbon isotopic content is present between rocks rich or poor in organic matter. Anderson and Arthur [31] and Dean et al. [33] mentioned that the organic matter $\delta^{13}C$ record in ancient sediments can be significantly influenced by diagenesis, bacterial reworking and changes in the availability of carbon to photosynthetic organisms. These processes might also have caused a change from the original carbon isotopic signature. Finally, the presence of organic matter (up to 3.2%) indicates that the Late Cre-

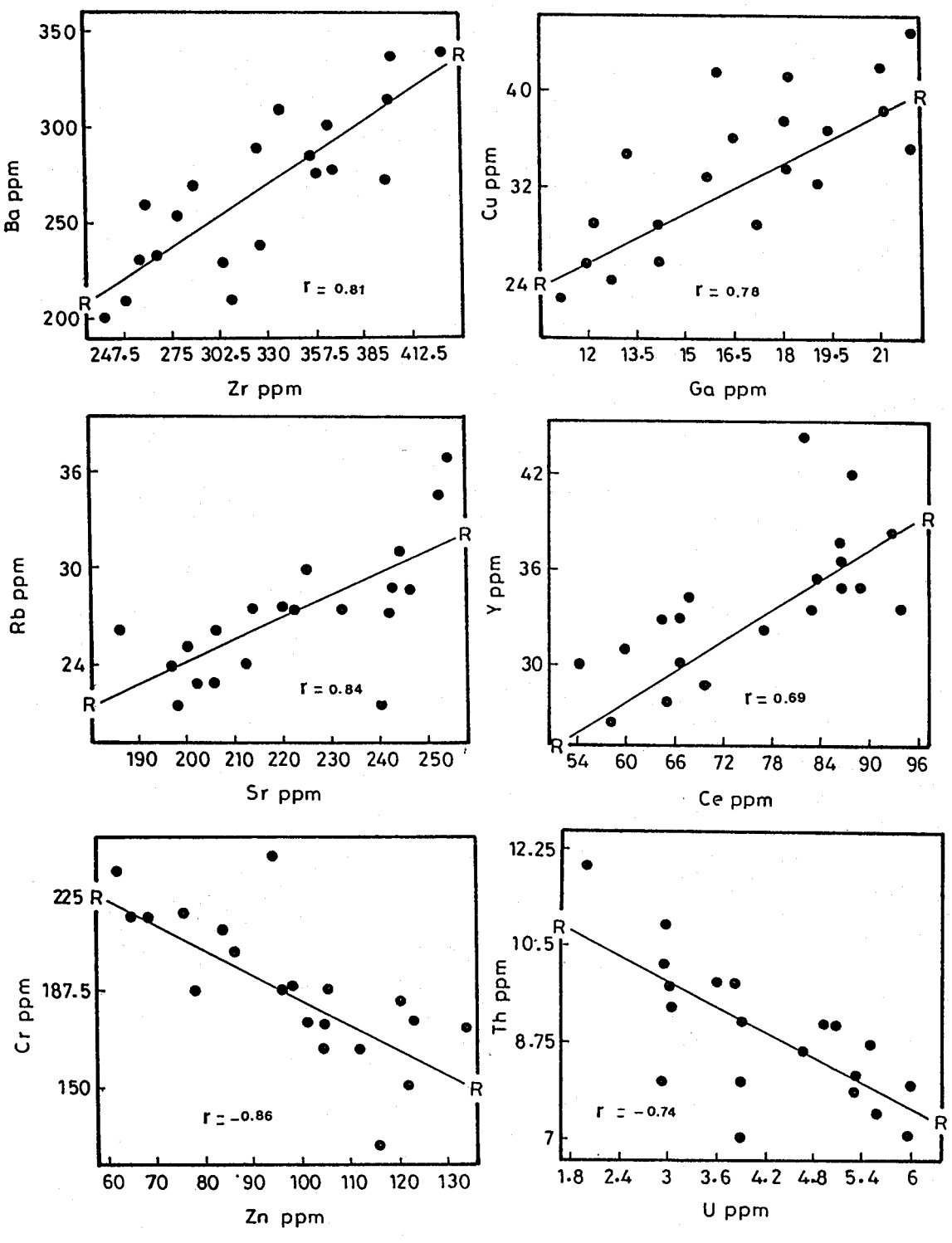

Figure 6. Trace element patterns in Upper Cretaceous black shales.

taceous did have the combination of a relatively high productive waters, contributions of continental material, rapid sedimentation, lack of dilution by clastics and/or anoxia conducive for accumulation of organic matter.

Pyrite:

Organic-rich sediments laid down in marine water environments are commonly characterized by diagenetic pyrite. The relationship between the pyritic sulfur and total organic carbon contents of these sediments have recently been discussed by Leventhal [34], Berner [8] and Berner and Raiswell [35-36]. However, their data are almost exclusively from fine clastic sediments in which availability of sulfate or metabolizable organic matter, but not Fe, is the controlling factor.

Regarding the present study samples, the following remarks are noticed

(1) Clustering of the pyrite crystals is commonly seen in the carbon-rich samples and discrete crystals occur in the relatively carbon-poor associations.

(2) Occurrence and textural features of the pyrite crystals in the black shales are in agreement with authigenic formation.

(3) There is a positive correlation between the TOC and total Fe (Fig. 7). This would emphasize the role of the organic matter, through bacterial action, on the formation of pyrite, since the presence of Fe^{++} is expected under such conditions. However, total Fe and TOC are sometimes correlated through an increasing clay fraction [10].

(4) The positive correlation between total Fe and S (Fig. 8) reflects the necessity of the SO^4 as sulfur donor species through reduction. That would easily be accomplished in the presence of organic matter.

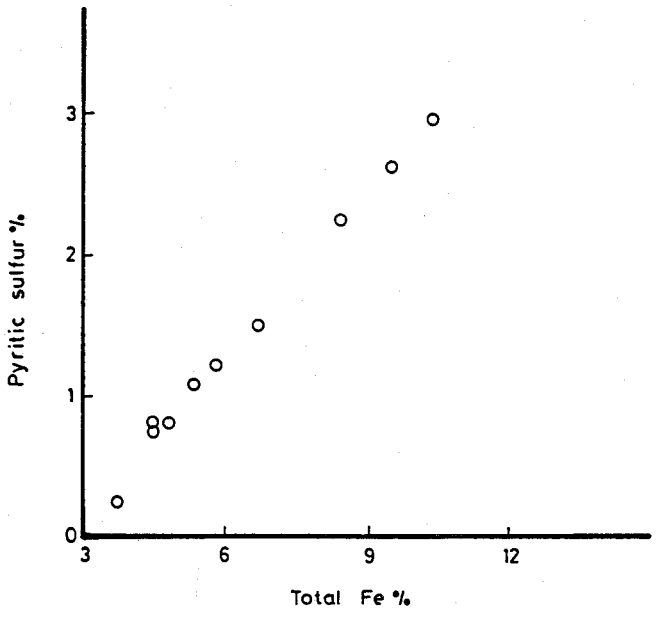

Figure 8. Total Fe and sulfur concentrations in Upper Cretaceous black shales.

(5) The total organic carbon vs sulphur relationship (Fig. 9) is of positive correlation. This might be due to thermal maturation effects [10].

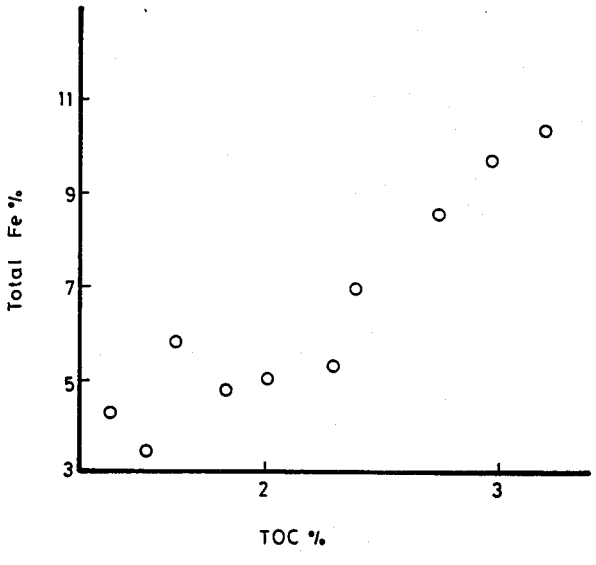

Figure 7. Total organic carbon and total Fe concentrations in Upper Cretaceous black shales.

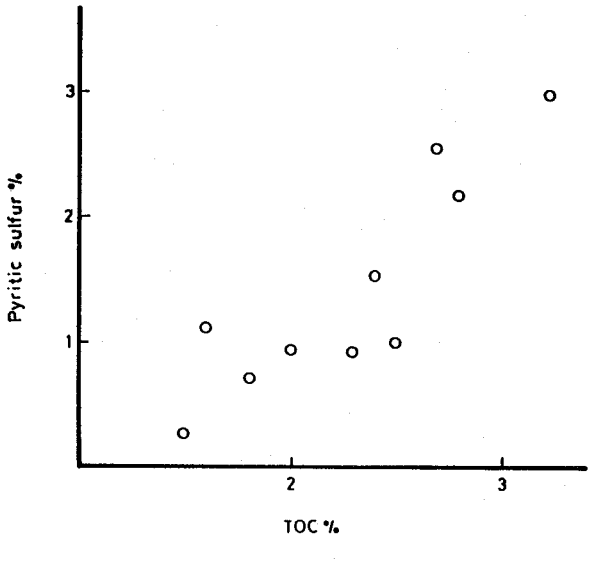

Figure 9. Total organic carbon and sulfur concentrations in Upper Cretaceous black shales.

The pyrite is detected as a minor constituent, of 1-4% abundance, in the black-shale bed of the Duwi Formation. It occurs commonly as euhedral crystals attaining 0.1 to 1.0 cm size, although some tiny globular forms (0.02 - 0.25 mm across) are occasionally seen in the C-rich samples. The pyrite crystals are erratically scattered in the enclosing bed, as discrete individuals and as clustered aggregates. The clustered pyrite crystals portray simple textures often of massive to mosaic-like appearance and are rarely twinned (Fig. 5A). Secondary pyrite growths are common, suggesting multiple stages of formation. Generally, these textural features are extremely constant on both vertical and lateral scales. The diagenetic origin of these pyrite crystals is a consequence of the burial evolution of the shale bed and algal and continental source is favoured to account for the carbonaceous material. This genetic appraisal lies principally upon the following:

1) Bacterial decay of the algae should provide the system with the necessary pre-requisites of pyrite formation (-Eh and HS^-) since the presence of Fe can not be excluded under such conditions.

2) The analyzed pyrite crystals (Table 2) are characterized by accommodating 4-7 ppm U and 2-10 ppm Th. These values are rarely recorded in pyrite crystals of hydrothermal origin [17]. The association of the pyrite crystals with the carbonaceous materials could account for this property.

3) The pyrite crystals contained Co ranging from 13 to 30 ppm and Ni from 29 to 52 ppm. The average Co/Ni ratio amounts to 0.47 which compares well with other published ones on diagenetic pyrite from some different districts [37].

4) The relative high contents of Ba, Sr, Rb and Cr (from 29 to 142, from 10 to 25, from 5 to 13 and from 13 to 30 ppm, respectively) might be attributed to slight contamination from the enclosing shale. These element contents do vary directly with percent of host-rock fragments included in the analyzed pyrite samples.

CONCLUSIONS

1) Three lithofacies have been defined in the Upper Cretaceous black shales: silt-rich mudstones, foraminifera-rich shales and clay-and organic matter-rich shales .

2) Smectite is the dominant clay mineral in the Upper Cretaceous black shales, regardless of sediment type.

3) Major elements (Si, Al, Mg and Ti) are present in slightly lower concentrations because of dilution by organic matter. In contrast, trace- element concentrations show a general enrichment pattern.

4) Organic matter is best preserved in areas of a basin where sediment accumulation rates are most rapid, organic-matter productivity is highest and bottom waters are anoxic. The carbon isotope ratios of Upper Cretaceous black shales (from -22 % to -28.7 %) suggest that marine source has contributed organic matter to these facies.

5) Occurrence, textural features and geochemical characteristics of the pyrite crystals in the black shale are in agreement with authigenic formation.

REFERENCES

[1] **Disnar, J.R.,** 1981. Etude experimental de la fixation de metaux par un materiau sedimentaire actual d'origine algaire. Geochim. Cosmochim. Acta, 45: 363-379.

[2] **Balistrieri, L.S. and J.W. Murray,** 1984. Marine scavenging: trace metal adsorption by interfacial sediment from MANOP Site H. Geochim. Cosmochim. Acta, 48: 921-929.

[3] **Graybeal, A.L. and G.R. Heath,** 1984. Rmobiliztion of transition metals in surficial pelagic sediments from the Eastern Pacific. Geochim. Cosmochim. Acta, 48: 965-975. Dissertation. Yale University. U.S.A.

[4] **Boyle, E.A., F. Sclater, and J.M. Edmond,** 1976. On the marine geochemistry of cadmium. Nature 263: 42-44.

[5] **Bruland, K.W.,** 1980. Oceanographic distributions of cadmium, zinc, nickel, and copper in the North Pacific. Earth Planet. Sci. Lett. 47: 176-198.

[6] **Collier, R.W. and J. Edmond,** 1984. The trace element geochemistry of marine particulate matter, Prog. Oceanogr. 13: 113-199.

[7] **Mossmann, J., A.C. Aplin, C.D. Curtis, and M. Coleman,** 1991. Geochemistry of inorganic and organic sulphur in organic-rich sediments from the Peru Margin. Geochim. Cosmochim. Acta, 55: 3581-3595.

[8] **Berner, R.A.,** 1984. Sedimentary pyrite formation: An update. Geochim. Cosmochim. Acta, 48: 605-615.

[9] **Boudreau, B.P.,** 1984. Diagenetic models of biologica processes in marine sediments. Ph. D. Thesis.

[10] **Raiswell, R. and R.A. Berner,** 1985. Pyrite formation in euxinic and semi euxinic sediments, Am. J. Sci., 285: 710-724.

[11] **Raiswell, R., F. Buchley, R.A. Berner, and T.F. Anderson,** 1988. Degree of pyritization of iron as paleo-environmental indicators of bottom-water oxygen, J. Sediment. Petrol, 58: 812-819.

[12] **Canfield, D.E.,** 1989. Reactive iron in marine sediments, Geochim. Cosmochim. Acta 53, 619-632.

[13] **Canfield, D.E.,** [1991] Sulfate reduction in deep-sea sediments, Am. J. Sci. 291: 177-188.

[14] **Emeis, K.C. and J.W. Morse,** 1990. Organic carbon, reduced sulfur, and iron relationships in sediments of the Peru Margin, ODP sites 680 and 688. Proc. ODP Sci. Repts. 112B: 441-454.

[15] **Berner, R.A.,** 1970. Sedimentary pyrite formation. Am. J. Sci. 268: 1-23.

[16] **Westrich, J.T. and R.A. Berner,** 1984. The role of sedimentary organic matter in bacterial sulfate reduction, Limnology and Oceanography 29: 236-249.

[17] **Gindy, A.R.,** 1961. Mineralization in phosphate Mine No. 5, (OM El Hewitat), Safaga District, Red Sea Province, U.A.R., Pan-Arab Science Congress Cairo, 575-594.

[18] **EL-Tarabili, E.,** 1969. Paleogeography, paleecology and genesis of the phosphatic sediments in the Quseir- Safaga area, U.A.R. Economic Geology, 64: 172-182.

[19] **Soliman, S.M. and K.M. Amer,** 1972. Petrology of the phosphorite deposits, Qusseir area, Egypt: Arab. Min. Petrol. Assoc. Trans., Cairo, Cong. Phosphate in A.R.E., 27: 17-48.

[20] **Glenn, C.R. and S. Mansour,** 1979. Reconstruction of the depositional and diagenetic history of phosphorites and associated rocks of the Duwi Formation (Late Cretaceou Eastern desert, Egypt: Ann. Geol. Surv. Egypt, IX: 388-407.

[21] **Ganz, H.,** 1987. Geochemical evaluation of hydrocarbon source rock characteristics and facies analysis-methods and application. Berliner Geowiss. Abh. 72.3: 669-690.

[22] **Germann, K., W.D. Bockr, H. Ganz, T. Schroter, and U. Troger,** 1987. Depositional conditions of Late Cretaceous phosphorites and black-shales in Egypt: Berl. Geowiss Abh., A. 75.3: 629-668.

[23] **Youssef, M.I.,** 1957. Upper Cretaceous rocks in Kosier area: Bull. Inst. Desert, Egypt, 7: 35-54.

[24] **Said, R.,** 1962. Geology of Egypt, Elsevier, Amsterdam, 377pp.

[25] **Boesen, C. and D. Postma,** 1988. Pyrite formation in anoxic environments of the Baltic, Am. J. Sci., 288: 575-603.

[26] **Norrish, K. and J.T. Hutton,** 1969. An accurate X-ray spectrographic method for the analysis of a wide range of geological samples, Geochim. Cosmochim. Acta, 33: 431- 453.

[27] **Ronov, A.B. and A.A. Migdisov,** 1971. Geochemical history of the crystalline basement and sedimentary cover of the Russian and North American platforms. Sedimentology, 16: 137-185.

[28] **Cameron, E.M. and R.M. Garrels,** 1980. Geochemical compositions of some Precambrian shales from the Canadian Shield. Chem. Geology, 28: 181-197.

[29] **Tourtelot, H.A.,** 1979. Black shale-its deposition and diagenesis. Clays and Clay Miner., 27: 313-321.

[30] **Calvert, S.E.,** 1976. The mineralogy and gechemistry of near-shore sediments. In J.P. Riley and R. Chester (eds.), Chemical Oceanography, 2nd ed. 6: 187-280.

[31] **Anderson, T.F. and M.A. Arthur,** 1983. Stable isotopes of oxygen and carbon and their application to sedimentologic and paleoenvironmental problems. In Arthur, M.A., Andeson, T.F. Kaplan I., R., Land, L.S., and Veizer, T., Stable Isotopes in Marine Geology: SEPM Short Course 10, 1-1-1-151.

[32] **Peterson, B.J., R.W. Howarth, and R.H. Garritt,** 1985. Multiple stable isotopes used to trace the flow of organic matter in estuarine food webs., Science, 227: 1361-1363.

[33] **Dean, W.E., M.A. Arthur, and G.E. Claypool,** 1986. Depletion of 13C in Cretaceous marine organic matter: source, diagenetic, or environmental signal Marine Geol., 70: 119-157.

[34] **Leventhal, J.S.,** 1983. An interpretation of the carbon and sulphur relationships in Black Sea sediments as indicators of environments of deposition. Geochim. Cosmochim. Acta, 47: 133-138.

[35] **Berner, R.A. and R. Raiswell,** 1983. Burial organic carbon and pyrite sulfur in sediments over Phanerozoic time: A new theory, Geochim. Cosmochim. Acta 47: 855-862.

[36] **Berner, R.A. and R. Raiswell,** 1984. C/S method for distinguishing freshwater from marine sedimentary rocks, Geology, 12: 365-368.

[37] **Cornwell, J.C. and J.W. Morse,** 1987. The chaacterization of iron sulfide minerals in marine sediments: Marine Chemistry, 22: 193-206.